ADP Ribosylation Factor and a 14-kD Polypeptide Are Associated with Heparan Sulfate–carrying Post-*trans*-Golgi Network Secretory Vesicles in Rat Hepatocytes

Walter Nickel,* Lukas A. Huber,‡ Richard A. Kahn,§ Nicola Kipper,* Andreas Barthel,* Dirk Fasshauer,* and Hans-Dieter Söling*

*Abteilung Klinische Biochemie, Zentrum Innere Medizin, Universität Göttingen, D-37070 Göttingen, FRG; ‡European Molecular Biology Laboratory, Cell Biology Programme, D-69012 Heidelberg, FRG; and §Laboratory of Biological Chemistry, National Cancer Institute, Bethesda, Maryland 20892

Abstract. Constitutive secretory vesicles carrying heparan sulfate proteoglycan (HSPG) were identified in isolated rat hepatocytes by pulse-chase experiments with [^{35}S]sulfate and purified by velocity-controlled sucrose gradient centrifugation followed by equilibrium density centrifugation in Nycodenz. Using this procedure, the vesicles were separated from plasma membranes, Golgi, *trans*-Golgi network (TGN), ER, endosomes, lysosomes, transcytotic vesicles, and mitochondria. The diameter of these vesicles was ~100–200 nm as determined by electron microscopy. A typical coat structure as described for intra-Golgi transport vesicles or clathrin-coated vesicles could not be seen, and the vesicles were not associated with the coat protein β-COP. Furthermore, the vesicles appear to represent a low density compartment (1.05–1.06 g/ml).

Other constitutively secreted proteins (rat serum albumin, apolipoprotein E, and fibrinogen) could not be detected in purified HSPG-carrying vesicles, but banded in the denser fractions of the Nycodenz gradient. Moreover, during pulse-chase labeling with [^{35}S]methionine, labeled albumin did not appear in the post-TGN vesicle fraction carrying HSPGs. These findings indicate sorting of HSPGs and albumin into different types of constitutive secretory vesicles in hepatocytes. Two proteins were found to be tightly associated with the membranes of the HSPG carrying vesicles: a member of the ADP ribosylation factor family of small guanine nucleotide–binding proteins and an unknown 14-kD peripheral membrane protein (VAPP14).

Concerning the secretory pathway, we conclude from these results that ADP ribosylation factor proteins are not only involved in vesicular transport from the ER via the Golgi to the TGN, but also in vesicular transport from the TGN to the plasma membrane.

FORMATION of constitutive secretory vesicles requires several intracellular vesicular transport steps, as well as the proper sorting of cargo proteins. Experiments performed in the yeast *Saccharomyces cerevisiae* have shown that secretion requires, among other gene products, the small guanine nucleotide–binding protein (SGBP)[1] Sec4p (Salminen and Novick, 1987). Subsequently, the Ypt1 gene product, another SGBP, has been shown to be required in the same yeast for the vesicular transport between ER and Golgi (Schmitt et al., 1988; Segev et al., 1988). In addition, the SGBPs ADP ribosylation factor (ARF) and Sar1 were found to be required in this step of the secretory pathway (Nakano and Muramatsu, 1989; Stearns et al., 1990). The involvement of SGBPs in functional control of the secretory pathway is also well established for mammalian cells (Zahraoui et al., 1989). The SGBPs rab1, rab2, rab6, and ARF were found to function in ER-Golgi and/or intra-Golgi transport (Balch et al., 1992; Chavrier et al., 1990; Goud et al., 1990; Haubruck et al., 1989; Schweizer et al., 1988; Taylor et al., 1992). Furthermore, SGBPs were also detected on early and late endosomes (Chavrier et al., 1990; Van der Sluijs et al., 1991), and their participation in the functional control of endosomal transport has been shown (Bucci et al., 1992; Lenhard et al., 1992). While the essential role of Sec4p for the final steps of secretion in yeast is documented, a similar role for a SGBP (rab8) in mammalian cells has been shown recently (Huber et al., 1993). In neuronal cells, the small GTP-binding protein rab3a can be found associated with the membranes of synaptic vesicles (Fischer von Mollard et al.,

Address correspondence to Hans-Dieter Söling, Abteilung Klinische Biochemie, Zentrum Innere Medizin, Universitat Gottingen, Robert Koch Str. 40, D-37070 Göttingen, FRG.

1. *Abbreviations used in this paper*: Apo E, apolipoprotein E; ARF, ADP ribosylation factor; dIgA, dimeric IgA; DPPIV, dipeptidylpeptidase IV; HSPG, heparan sulfate proteoglycan; SGBP, small guanine nucleotide-binding protein; TGN, *trans*-Golgi network.

1990). Upon stimulation of neurosecretion, rab3a dissociates from the synaptic vesicles and appears intermittently associated with the plasma membrane (Fischer von Mollard et al., 1991). After retrieval of the empty synaptic vesicles from the presynaptic membrane, the refilling of the vesicles seems to be associated with a reattachment of rab3a to the vesicular membrane (Cameron et al., 1991; Maycox et al., 1992; Südhof and Jahn, 1991).

Post-*trans*-Golgi network (TGN) secretory vesicles from mammalian cells were first isolated from Madin-Darby canine kidney cells (Bennett et al., 1988; Wandinger-Ness et al., 1990). Two proteins could be identified that are highly enriched in this type of transport vesicle. The small GTPase rab 8 (Huber et al., 1993) and a membrane protein of 21 kD (VIP21, Kurzchalia et al., 1992). Exocytic transport vesicles generated in vitro from the *trans*-Golgi network were immunoisolated and shown to contain a mixture of mature secretory and plasma membrane proteins (Salamero et al., 1990). In addition, post-TGN transport vesicles carrying heparan sulfate could be identified in rat hepatocytes (Graham and Winterbourne, 1988), but they were not isolated and characterized concerning protein components.

We have, therefore, purified constitutive secretory vesicles from isolated rat hepatocytes in an attempt to characterize the proteins associated with them. In addition, we investigated whether the constitutive secretory pathway involves post-TGN sorting processes or not.

Using ^{35}S-sulfated heparan sulfate proteoglycan (HSPG) as a marker, we could identify a vesicular carrier functionally located between the TGN and the plasma membrane. An SGBP and a 14-kD non-GTP binding protein were found to be associated with the membranes of the vesicles described. The SGBP was identified as a member of the ARF family of SGBPs.

Moreover, we present results which indicate that HSPGs on one hand and albumin on the other hand are sorted into different post-TGN secretory vesicles.

Materials and Methods

1D9 is a mouse monoclonal antibody to ARF1. The mouse monoclonal anti-β-COP antibody and the polyclonal anti-TGN-38 antibody were the generous gifts of Dr. Thomas Kreis (Dept. of Cell Biology, University of Geneva, Sciences II, Geneva, Switzerland) and Dr. Paul Luzio (University of Cambridge, Dept. of Clinical Biochemistry, Addenbrooke's Hospital, Cambridge, United Kingdom), respectively. A polyclonal antibody directed against dipeptidylpeptidase IV (DPPIV) was a kind gift of Dr. Werner Reutter (Freie Universität Berlin, Institut fur Molekularbiologie und Biochemie, Berlin, Germany). Polyclonal antibodies recognizing the ER-resident calcium-binding proteins CaBP1, calreticulin (CaBP3), and grp94 (CaBP4) were supplied by Dr. Phuc Nguyen Van (Abteilung Klinische Biochemie, Universität Göttingen). Polyclonal antibodies directed against the following secretory proteins were from commercial sources: rat serum albumin (RSA) (Nordic Immunology, Tilburg, The Netherlands), rat fibrinogen (Paesel, Frankfurt/Main, Germany), and human apolipoprotein E (apo E) (Greiner, Frickenhausen, Germany).

Isolation of Rat Hepatocytes and Metabolic Labeling Using [^{35}S]sulfate and [^{35}S]methionine

Isolation of rat hepatocytes was performed according to a modification (Seglen, 1974) of the method of Berry and Friend (1969).

For metabolic labeling with [^{35}S]sulfate, the cells (150 mg/ml wet wt) were preincubated at 37°C for 30 min in incubation medium (NaCl 116 mM, $NaHCO_3$ 26 mM, glucose 6 mM, NaH_2PO_4 1 mM, $CaCl_2$ 1.8 mM, KCl 5.4 mM, $MgCl_2$ 0.8 mM, heparin 12 U/ml) in the presence of 95% O_2 and 5% CO_2. After a temperature shift to 32°C, 1 mCi/ml carrier-free [^{35}S]sulfate (24.3–40.5 Ci/mg S; Amersham-Buchler, Braunschweig, Germany) was added. Pulse and chase (using 5 mM Na_2SO_4, final concentration) times were as indicated. Alternatively, cells were labeled in incubation medium using [^{35}S]methionine (>1,000 Ci/mmol, 100 μCi/ml; Amersham-Buchler). In these experiments, incubation medium was supplemented with an amino acid mixture (0.1 mM each) lacking methionine. Pulse and chase (using 2 mM methionine) times were as indicated in the figure legends.

Subcellular Fractionation

Cells (300 mg wet wt) were homogenized with the fivefold volume (vol/wt) of 0.3 M sucrose containing 20 mM Tris-HCl (pH 7.4 at 4°C), 1 mM benzamidine, and 20 μg/ml PMSF by applying 20 strokes with a "tight-fitting" Dounce homogenizer (Braun, Melsungen, Germany). After centrifugation for 10 min at 1,000 *g*, the supernatant was loaded onto a 10% to 35% (wt/wt) continuous sucrose gradient in 10 mM Hepes, pH 7.2. After centrifugation for 15 min at 106,000 g_{max} in a swing-out rotor (SW41; Beckman Instruments, Inc., Fullerton, CA), the gradient was fractionated into 23 portions of 500 μl. The first five fractions (2.5 ml) from the top of the gradient were combined and then loaded onto a continuous 20 to 35% (wt/vol) Nycodenz gradient in 20 mM Tris-HCl (pH 7.4 at 4°C), 1 mM $MgCl_2$, 1 mM $CaCl_2$, and 2.5% (wt/wt) sucrose. After equilibrium centrifugation for 20 h at 154,000 g_{max} in the SW41 swing-out rotor, the gradient was fractionated as given above.

For the preparation of post-TGN vesicles processed for electron microscopy, the purification protocol was upscaled. Sucrose and Nycodenz gradient centrifugations were performed using the SW28 swing-out rotor. The gradients were formed by the solutions mentioned above. The total volume was 34 ml (sucrose) and 30 ml (Nycodenz), respectively. Cells (1 g) were processed as given above. The gradients were fractionated into portions of 1 ml. Fractions 1–8 from the top of the sucrose gradient were loaded onto the Nycodenz gradient.

Where mentioned, the fractions were diluted with the twofold volume of PBS and spun for 2 h at 100,000 *g* to sediment particulate fractions.

Determination of Marker Enzymes

UDP-galactosyltransferase activity was determined according to Verdon and Berger (1983), asialofetuin sialyltransferase according to Posner et al. (1985), β-hexosaminidase according to Hall et al. (1978), alkaline phosphodiesterase according to Arouson and Trouster (1974), succinate dehydrogenase according to Brdicka et al. (1968), and potassium-dependent phosphatase according to Arvan and Castle (1982). The transferrin receptor was detected by internalization of [^{125}I]transferrin for 15 min at 37°C using isolated rat hepatocytes grown on cell culture dishes.

Quantification of ^{35}S-labeled Macromolecules

Aliquots (≤100 μl) of the fractions obtained from the sucrose- and Nycodenz gradients were assayed by precipitation of macromolecules using cetylpyridinium chloride (Graham and Winterbourne, 1988).

Treatment of Particular Fractions with Proteinase K and Electrophoresis of ^{35}S-labeled Proteoglycans

Fractions 1–3 from the top of the Nycodenz gradient were pooled, and aliquots (50 μl) were incubated with 1 mM dibucaine (Scheele et al., 1980) for 5 min at 4°C. Subsequently, 0.1 mg/ml proteinase K and 0.3% Triton X-100 were added as indicated. The digestion (30 min at 4°C) was stopped by adding 2 mM PMSF. Subsequently, macromolecules were precipitated using acetone and resuspended in sample buffer (Carney et al., 1986). The samples were boiled and then analyzed on 1.2%/0.6% polyacrylamide-agarose composite gels (Carney et al., 1986). ^{35}S-labeled proteoglycans were visualized by fluorography (Carney et al., 1986).

Immunoblotting for Marker Antigens

After SDS-PAGE (Laemmli, 1970) and blotting onto nitrocellulose, CaBP1, calreticulin, grp94, TGN38, apo E, RSA, fibrinogen, and dipeptidylpeptidase IV (DPPIV) were detected with monospecific polyclonal rabbit antisera and peroxidase-conjugated goat anti-rabbit antibodies, β-COP and ARF1 with monoclonal mouse antibodies and peroxidase-conjugated goat anti-mouse antibodies. The detection of peroxidase was with diaminobenzidine hydrochloride as substrate.

Internalized biotinylated dimeric IgA (dIgA) was measured after isolated rat liver perfusion at 37°C for 13 min (3 min pulse, 10 min chase) (Hoppe et al., 1985). After SDS-PAGE under nonreducing conditions and blotting onto nitrocellulose, the biotinylated dIgA was detected using a chemiluminescence system (Photo-blot™; Gibco BRL, Eggenstein, Germany).

GTP[γ^{35}S] and GTP[α^{32}P] Ligand Binding

Samples were subjected to 13% SDS-PAGE followed by electrophoretic transfer onto nitrocellulose in 25 mM Tris (pH 8.4), 100 mM glycin, and 20% methanol. The membrane was immediately rinsed with binding buffer (50 mM NaH_2PO_4, pH 7.5, 10 mM $MgCl_2$, 2 mM DTT, 0.3% Tween 20, 4 mM ATP) and incubated twice for 10 min again in binding buffer. The membrane was subsequently incubated in the same buffer containing 2 μCi/ml GTP [γ^{35}S] (specific activity = 1,200 Ci/mmol) or 2 μCi [α^{32}P]-ATP (specific activity = 3,000 Ci/mmol) for 2 h. Unbound radioactive GTP was separated by washing the membrane six times for 5 min with binding buffer. The blot was dried and exposed for 48 h to an x-ray film.

Two-dimensional gel electrophoresis, transfer to nitrocellulose blots, and [α^{32}P]GTP overlay were performed as described (Celis et al., 1990; Huber and Peter, 1993; Huber et al., 1993).

Electron Microscopy

Membranes were sedimented by ultracentrifugation (100,000 *g*, 2 h) and treated with Karnovsky fixative. The pellets were then washed with 0.1 M sodium cacodylate (pH 7.3) and subsequently overlayed with 2% OsO_4 in 0.05 M sodium cacodylate. After washing three times with 0.1 M sodium cacodylate (pH 7.3), the pellet was treated with increasing concentrations of ethanol (≤100%). After treatment with propylenoxide and a mixture of propylenoxide/Epon, the pellet was finally embedded in Epon. After polymerization (overnight, 60°C), ultra-thin sections were obtained and again contrasted by treatment with 1.5% uranylacetate and 3% Pb-citrate. Negative-stained images were obtained as described by Robinson et al. (1985).

Results

Characterization of the Velocity Sucrose Gradient

The results are presented in Fig. 1, *A* and *B*. The bottom fractions contain most of the sialyltransferase and the β-hexosaminidase activities, as well as all activity of Na^+/K^+-ATPase (measured as K^+-dependent phosphatase). The bottom fraction, therefore, contains lysosomes, all plasma membranes, and the TGN. One should stress the point that the peak activity for the Golgi marker UDP-galactosyltransferase is clearly separated from the peak activity of sialyltransferase, supporting the concept that the sialyltransferase reaction does occur mainly in the TGN and not in the

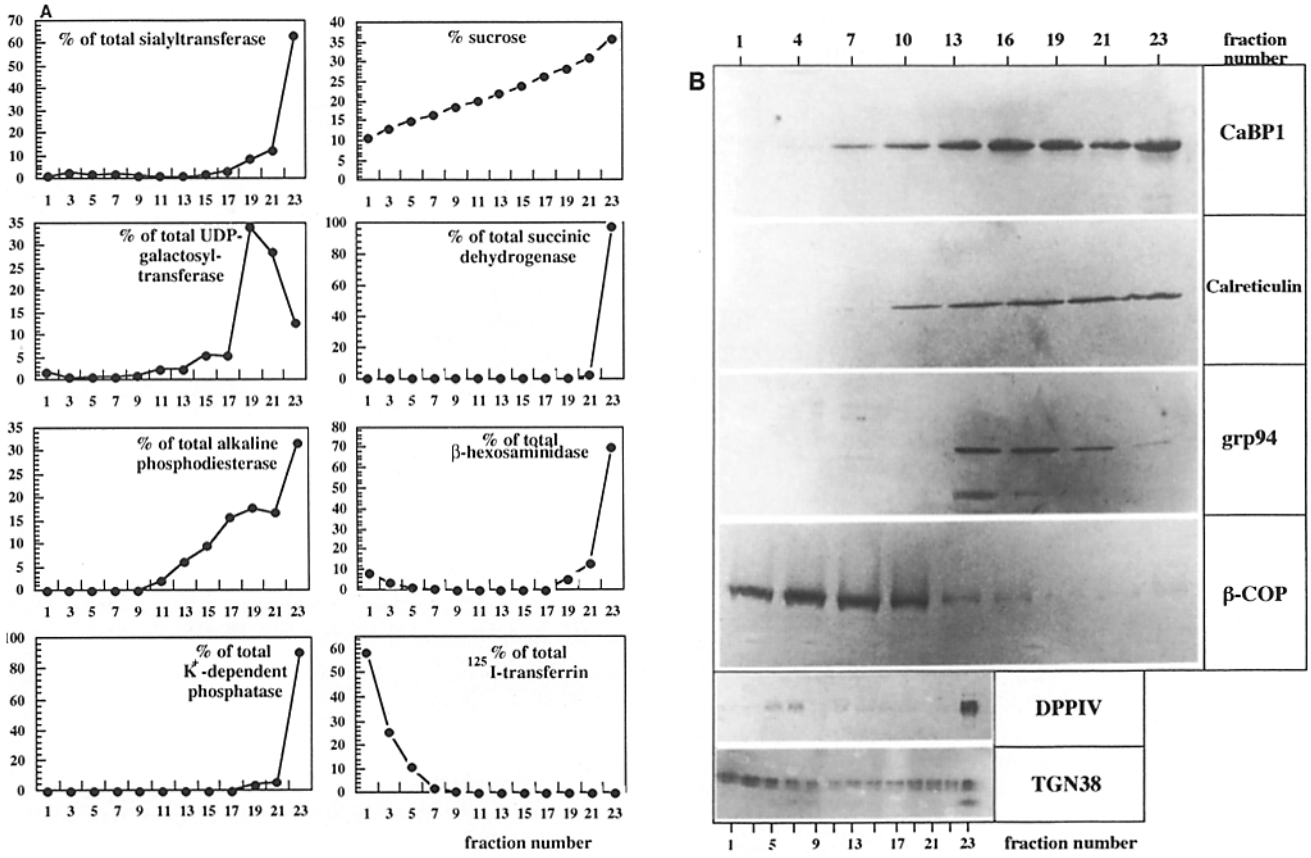

Figure 1. (*A*) Distribution of subcellular marker enzymes in the velocity-controlled sucrose gradient and corresponding sucrose density. A 10–35% (wt/wt) continuous sucrose gradient was used as described under Materials and Methods. Fraction 1 is the uppermost fraction, and fraction 23 the bottom fraction. 300 mg (wet wt) of hepatocytes were used per gradient. Homogenization and subcellular fractionation was performed as described in Materials and Methods using a Beckman SW41 swing-out rotor. Aliquots from the fractions indicated were analyzed by the procedures listed under Materials and Methods. The sum of enzyme activities in all fractions was taken as 100%. Sucrose density was determined by refractometry. (*B*) Distribution of subcellular marker antigens in the velocity-controlled sucrose gradient. The experimental procedures were identical to that described in the legend of (*A*). Aliquots from the indicated fractions of the gradient were diluted and particulate material sedimented by ultracentrifugation (100,000 *g*, 2 h) as given in Materials and Methods. The sedimented material was processed by SDS-PAGE and immunoblotting (see Materials and Methods) according to standard procedures.

trans-Golgi cisternae. Alkaline phosphodiesterase, a marker for the apical plasma membrane, is spread over the whole lower part of the gradient. Endocytosed [^{125}I]transferrin appears on the top of the gradient, where also ~10% of β-hexosaminidase could be found. The appearance of some β-hexosaminidase activity in the top fractions was a consistent finding. This portion of β-hexosaminidase represents, most likely, enzyme acitivity in late endosomes in transit to lysosomes.

The markers for the endoplasmic reticulum (CaBP1, calreticulin, and grp94) (Peter et al., 1992) were observed in fractions 7–23 (Fig. 1 *B*), whereas the coat protein β-COP appeared in the upper part of the gradient. The TGN marker protein TGN38 (Luzio et al., 1990) appeared throughout the gradient, indicating that this protein is not restricted to the TGN, but circulates between TGN and the plasma membrane (Reaves et al., 1993). DPPIV is observed in the bottom fraction (representing enzyme in plasma membrane sheets), as well as in fraction 5–7, most likely representing enzyme associated with small plasma membrane vesicles generated by disrupted plasma membrane sheets.

Identification of Secretory Vesicles Carrying ^{35}S-sulfated Macromolecules

Sulfation of proteins and proteoglycans is a TGN-specific posttranslational modification (Baeuerle and Huttner, 1987; Kimúra et al., 1984). The transport of sulfated proteins between the TGN and the plasma membrane can be followed by pulse-chase experiments with [^{35}S]sulfate (Tooze and Huttner, 1990). After a short pulse, the chase time-dependent distribution of labeled macromolecules in the sucrose velocity gradient allows the identification of post-TGN transport vesicles. To diminish the risk that radioactive protein appeared in post-TGN vesicles already during the 4-min pulse, we performed the experiments at 32°C instead of 37°C. At the lower temperature, the kinetics of transport between TGN and plasma membrane were slowed down, thus making it easier to identify a post-TGN transport vesicle. After a 4-min pulse, almost 100% of ^{35}S-labeled macromolecules appeared together with the peak of sialyltransferase (Fig. 2) at the bottom of the sucrose gradient (Fig. 1 *A*). As shown in Fig. 3, the ^{35}S-labeled macromolecules represent almost exclusively heparan sulfate proteoglycan. After 4 min of chase, ~50% of the ^{35}S-labeled macromolecules had shifted to the top of the gradient, which was devoid of marker enzymes for the plasma membrane (alkaline phosphodiesterase; K^+-dependent phosphatase) or the TGN (sialyltransferase) (Fig. 1 *A*). After 8 min of chase, the main portion of ^{35}S-labeled macromolecules appeared in the top fractions of the sucrose gradient (Fig. 2). After 12 and 30 min of chase, an increasing portion of ^{35}S-labeled macromolecules had returned to the bottom of the gradient. The transport of HSPGs from the TGN to the cell surface does not involve the endocytic compartments (Graham and Winterbourne, 1988). Therefore, the fraction of labeled macromolecules appearing in the bottom fractions of the gradient after 12 and 30 min of chase represents HSPGs, which had reached the cell surface. Accordingly, the ^{35}S-labeled macromolecules on top of the gradient (4 min pulse, 8 min chase) are located within constitutive secretory vesicles, rather than vesicles directed to endosomes or lysosomes. The ^{35}S-labeled macromolecules appearing in the top fractions of

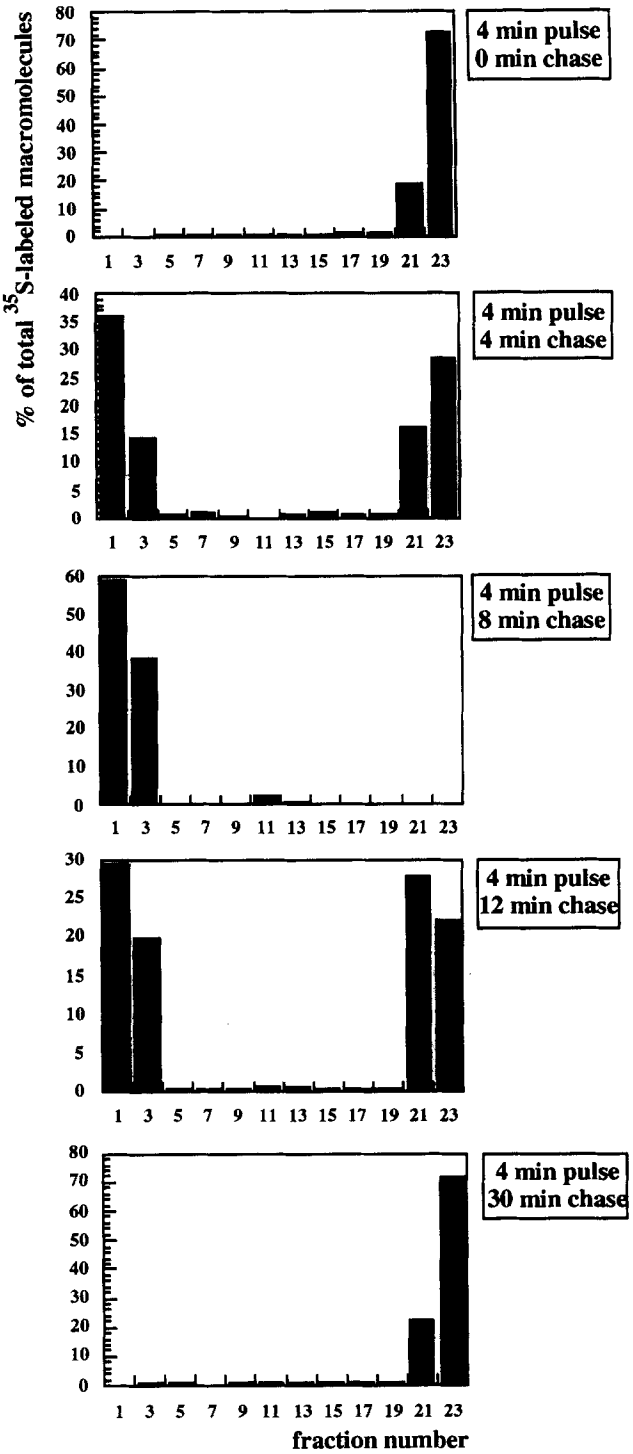

Figure 2. Time-dependent distribution of ^{35}S-labeled macromolecules in a velocity-controlled sucrose gradient after pulse-chase labeling with [^{35}S]sulfate. Hepatocytes (150 mg wet wt/ml, 2 ml total per experimental condition) were depleted of endogenous sulfate by incubation for 30 min at 37°C in sulfate-free medium (see Materials and Methods). The suspension was then transferred to 32°C and pulse labeled for 4 min with [^{35}S]sulfate (1 mCi/ml). The chase period was started by addition of 5 mM (final concentration) sodium sulfate at 32°C for the times indicated. Subsequently, cells were kept on ice to prevent any intracellular transport. Homogenization and subcellular fractionation by velocity-controlled sucrose centrifugation was as described in the legend to Fig. 1. Incorporation of radiolabeled sulfate into macromolecules was determined by precipitation using cetylpyridinium chloride (see Materials and Methods).

the gradient after chasing for 8 min are located within membrane-enclosed vesicles, as they were found to be resistant to proteinase K unless detergent was included (Fig. 3). It appears, therefore, that the top fractions of the sucrose gradient, which contain most of the ^{35}S-labeled macromolecules after 8 min of chase, represent a vesicular compartment functionally located between the TGN and the plasma membrane; i.e., they represent constitutive secretory vesicles.

Nature of the ^{35}S-sulfated Macromolecules

Upon electrophoresis of homogenates from ^{35}S-sulfated cells in a composite polyacrylamide/agarose gel, ^{35}S-sulfated macromolecules appeared primarily as a single band (Fig. 3). The labeled macromolecule was of the heparan sulfate type, since it was sensitive to digestion with heparinase II (Fig. 3).

Nycodenz Gradient Centrifugation

To further purify the post-TGN vesicle fraction containing the ^{35}S-labeled HSPGs (4 min pulse, 8 min chase), fractions 1–5 of the sucrose gradient were combined, loaded on to a Nycodenz gradient, and spun and processed as described in Materials and Methods. As given in Fig. 4 *A*, the ^{35}S-labeled HSPGs were restricted to the first three top fractions (peak in fraction 2) of this gradient. The fractions containing most of the [^{125}I]-transferrin and β-hexosaminidase activity, indicative of endosomes, appeared in fractions 5–9 and 5–7, respectively. The distribution of marker antigens is shown in Fig. 4 *B*. The coat protein β-COP was recovered from fractions 11–17. DPPIV was distributed between fractions 5 and 9. DPPIV appearing in fractions 7–9 moved further down during SDS-PAGE than in the species mainly observed in fraction 5. This represents most likely differences in the glycosylation pattern. Fractions 7–9 more-

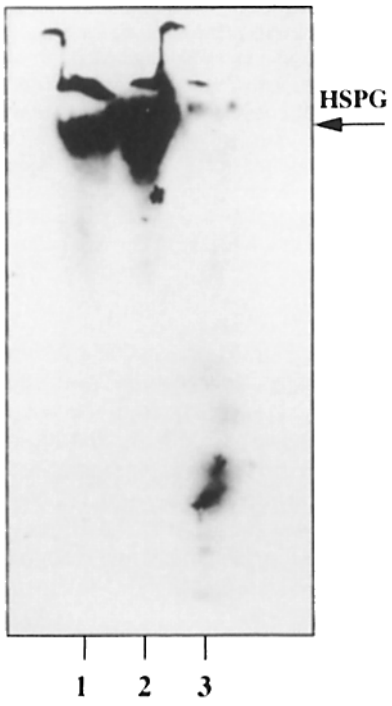

Figure 3. Digestion of ^{35}S-labeled macromolecules with heparinase II. Hepatocytes (150 mg wet wt/ml) were depleted of endogenous sulfate for 30 min at 37°C in incubation medium (see Materials and Methods). The cells were then labeled in the presence of 1 mCi/ml [^{35}S]sulfate for 15 min at 37°C. The cells were kept on ice and homogenized as described in Materials and Methods. The total volume was 1 ml. Homogenate (20 μl) was either precipitated directly with cold acetone (−20°C) and processed by polyacrylamide/agarose gel electrophoresis (lane *1*), or acetone precipitation and electrophoresis was performed with 50 μl homogenate each after incubation for 16 h at 25°C in the absence (lane *2*) or presence (lane *3*) of 2.5 U heparinase II. The dried gels were autoradiographed for 2 d.

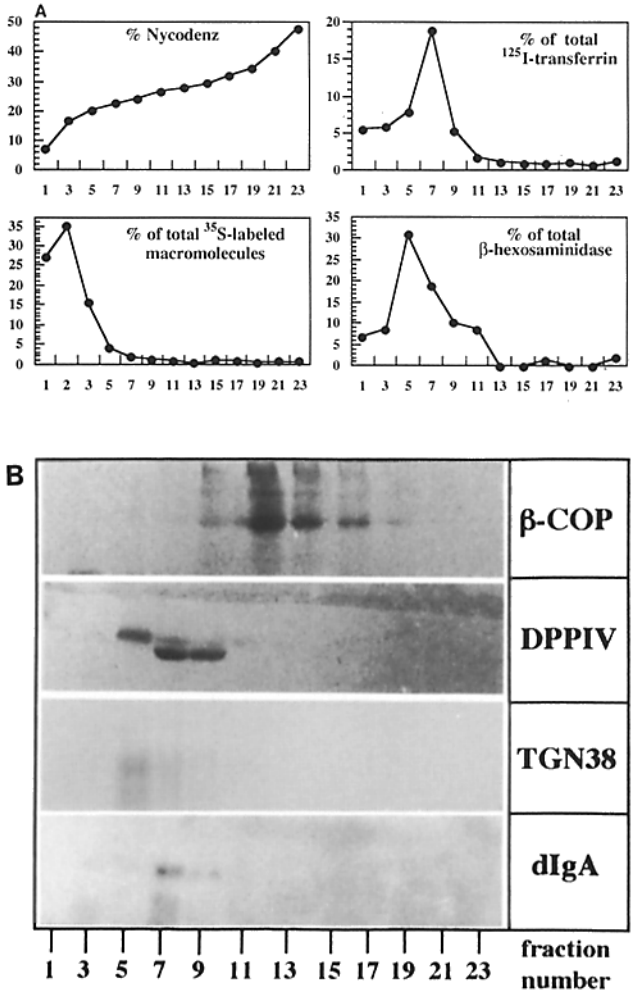

Figure 4. (*A*) Density distribution and distribution of subcellular marker proteins in the Nycodenz gradient. Fractions 1–5 of the velocity-controlled sucrose gradient (Fig. 1) were pooled and loaded onto a 20–35% (wt/vol) Nycodenz gradient using a Beckman SW41 swing-out rotor. Aliquots of the fractions indicated were analyzed by the procedures listed under Materials and Methods. The sum of the specific proteins in all fractions was set to 100%. Nycodenz density was determined by refractometry. (*B*) Distribution of subcellular marker antigens in the Nycodenz gradient. Experimental procedures were identical to that described in the legend of *A*. Aliquots from the indicated fractions of the gradient were diluted 1:2 (vol/vol) with phosphate-buffered saline and particulate material sedimented by ultracentrifugation (100,000 *g*, 2 h). The sedimented material was processed by SDS-PAGE and immunoblotting (see Materials and Methods) according to standard procedures.

over contained also internalized dIgA. The fact that internalized [^{125}I]-transferin, β-hexosaminidase, and dIgA banded together in fractions 5–9 indicates that in the Nycodenz gradient, these fractions contain endocytic compartments including transcytotic vesicles. DPPIV most likely represents small plasma membrane vesicles. As shown in Fig. 1 *B*, TGN38 was not only found in the TGN fractions of the velocity-controlled sucrose gradient but also in the vesicular top fractions. In fact, TGN38 was also reported to cycle between plasma membrane and endosomal compartments (Reaves et al., 1993). Fraction 5 of the final Nycodenz gradient contained TGN38, whereas no TGN38 was observed in the fractions containing ^{35}S-labeled HSPGs (fractions 1–3). TGN38 is, therefore, most likely associated with endosomes and plasma membrane vesicles, since it seems unlikely that TGN38 is associated with small vesiculated TGN fragments artificially produced during the homogenization procedure, because in this case, the fraction should also contain sialyltransferase activity and early labeled proteoglycan (4-min pulse without chase). However, in looking at Figs. 1 *a* and 2, it is clear that fractions 1–5 of the sucrose gradient, which were subsequently used for the Nycodenz equilibrium density centrifugation, neither contain measurable amounts of sialyltransferase nor early labeled proteoglycans.

The constitutive secretory vesicles are a low density compartment as the ^{35}S-labeled proteoglycan (4 min pulse, 8 min chase) appeared in the top fractions of the Nycodenz gradient. The density of the vesicles was estimated to be 1.05–1.06 g/ml. These data fit well with those reported earlier for HSPG-carrying secretory vesicles from rat hepatocytes (Graham and Winterbourne, 1988).

HSPG Carrying Secretory Vesicles Remain Intact during Purification

About 75% of the ^{35}S-labeled HSPGs (fractions 1–3 of the Nycodenz gradient) could be sedimented by ultracentrifugation (Fig. 5 *A*). The remaining 25% of labeled proteoglycans appeared in the supernatant. This most likely represents incomplete sedimentation of vesicles as the ^{35}S-labeled HSPGs were resistant to digestion with proteinase K unless Triton X-100 had been added (see below).

Proteinase K failed to digest the proteoglycans, unless Triton X-100 was included (Fig. 5 *B*). After addition of 0.3% Triton X-100, the labeled proteoglycan became completely digested within 10 min. These results indicate that the ^{35}S-labeled HSPGs are protected by a vesicular structure.

Electron Microscopy of HSPG-carrying Post-TGN Vesicles

To obtain electron micrographs, the purification procedure of HSPG-carrying vesicles was scaled up by using a Beckman SW28 rotor. The amounts of hepatocytes and the preparation of the gradients were as described in Materials and Methods. The determination of subcellular markers revealed that the degree of vesicle purity was identical compared to the fractionation procedure described above (data not shown). Fig. 6 shows electron micrographs of HSPG-carrying vesicles. In *A*, negative stains are shown, while *B* shows an image obtained from ultra-thin sections. The diameter of the vesicles ranged from ~100–200 nm. Otherwise the vesicles appeared remarkably homogenous. In contrast to Golgi-

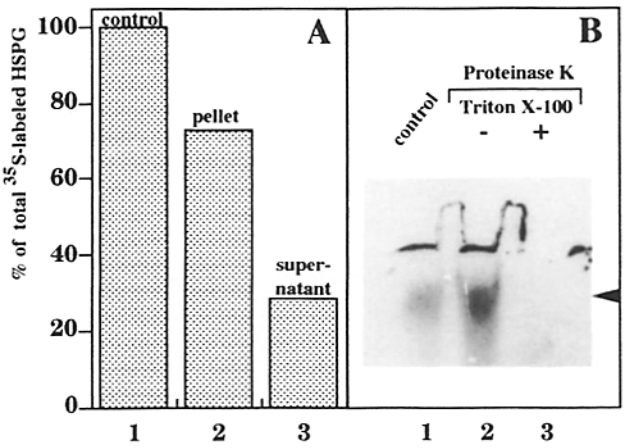

Figure 5. ^{35}S-sulfated HSPGs (4 min pulse, 8 min chase) are located within membrane-enclosed vesicles. (*A*) Purified post-TGN vesicles carrying HSPGs (fractions 1–3, Nycodenz gradient, SW41 swing-out rotor) were diluted and sedimented by ultracentrifugation at 100,000 *g* for 2 h. Radiolabeled proteoglycan was detected in both sediment and supernatant by precipitation using cetylpyridinium chloride as described under Materials and Methods. Up to 25% of the [^{35}S]HSPGs were found in the supernatant, while >75% were recovered in the sediment. (*B*) Protection of ^{35}S-labeled HSPG against proteolysis. Fractions 1–3 of the Nycodenz gradient (SW41 swing-out rotor) were combined (total volume = 1.5 ml) and incubated with 1 mM dibucaine for the stabilization of membranes as described under Materials and Methods. Lane *1*, 20 μl of the combined fractions were incubated without addition of protease; lane *2*, 50 μl of the combined fractions were incubated with proteinase K (0.1 mg/ml final concentration) for 30 min at 4°C; lane *3*, 50 μl of the combined fractions were incubated with proteinase K (0.1 mg/ml) in the presence of 0.3% (vol/vol) Triton X-100 for 30 min at 4°C. Macromolecules were precipitated with cold acetone and analyzed on polyacrylamide/agarose composite gels followed by fluorography. The gels were dried and exposed to an x-ray film (8–10 d).

derived vesicles (Malhotra et al., 1989), the vesicles shown in Fig. 6 did not exhibit a detectable coat structure. The same results were obtained when vesicles were fixed in the presence of tannic acid (data not shown). It may be that these vesicles had lost their coat structure during the preparation, as in contrast to the preparation of Golgi-derived vesicles (Malhotra et al., 1989), they were prepared in the absence of GTPγS, which is known to inhibit the uncoating reaction because it inhibits the GTPase reaction of small GTP-binding proteins.

Characterization of HSPG-carrying Post-TGN Vesicles

Fractions 1–6 of the Nycodenz gradient were diluted with PBS and sedimented by ultracentrifugation. The sedimented proteins were separated by SDS-PAGE and silver stained (Fig. 7). The most prominent proteins had apparent molecular masses of ~14 and 30 kD, respectively. While the 14-kD protein was always colocalized with the ^{35}S-labeled HSPG (4 min pulse, 8 min chase) in fractions 1–3, the 30-kD protein drifted in some experiments to fractions of higher density. It remains, therefore, unclear, whether the 30-kD protein is a true component of this vesicle population.

To determine the membrane association of the 14-kD protein the following experiments were performed (data not

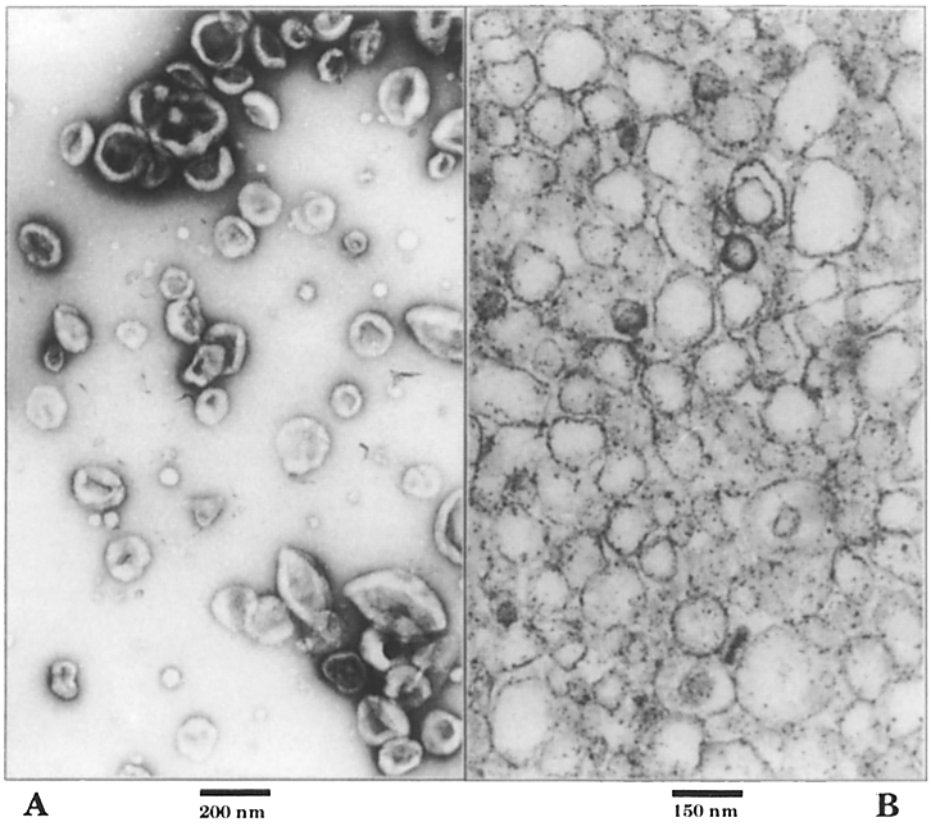

Figure 6. Electron microscopy of TGN-derived secretory vesicles. For electron microscopy, isolated hepatocytes (corresponding to about 1 g wet wt) were homogenized as described under Materials and Methods. Subcellular fractionation by velocity-controlled sucrose centrifugation was performed using a Beckman SW28 swing-out rotor (see Materials and Methods). Fractions 1–8 (1 ml/fraction) of the sucrose gradient were combined, loaded onto the Nycodenz gradient (again using the Beckman SW28 swing-out rotor) and spun for 20 h at 150,000 g_{av} (for details, see Materials and Methods). The fractions 1–12 (total volume = 12 ml) of this gradient contained ^{35}S-sulfated HSPGs (4 min pulse, 8 min chase), with a peak in fractions 4–6. According to biochemical characterization, the purity of the vesicles obtained was comparable to that of vesicles obtained during small scale purifications using the SW41 rotor. Therefore, the combined fractions 4–6 of the gradient were used for the preparation of electron micrographs as described under Materials and Methods. (*A*) Negative staining; (*B*) ultra-thin sections. The dark dots in *B* represent artificial precipitates.

shown). The 14-kD protein was partially extracted (~50%) by hypotonic extraction with 1 mM $NaHCO_3$ (pH 8.4), whereas 1 M NaCl removed almost 80–90% of the protein from the vesicles. Under strong alkaline extraction conditions (100 mM Na_2CO_3, pH 11.6) the 14-kD protein was completely extracted from the vesicles. Finally, when the 14-kD protein was subjected to Triton X-114 phase partitioning, the protein was quantitatively recovered in the water phase. When intact vesicles were incubated with proteinase K, the 14-kD protein became digested without addition of detergent. Accordingly, we conclude that the 14-kD protein is peripherally attached to the membrane of the HSPG-carrying post-TGN vesicles. Therefore, the protein was designated VAPP14 (vesicle associated peripheral protein of molecular mass 14 kD).

The Small GTP-binding Protein ARF is Associated with HSPG-Carrying Vesicles

Since the small GTP-binding protein ARF has been found to be involved in several types of intracellular vesicular transport, we have analyzed the fractions of the sucrose and the Nycodenz gradients for the presence of ARF. All fractions from the two gradients were diluted with PBS, and the vesicular structures were sedimented by ultracentrifugation, as indicated in Materials and Methods. The sedimented material was analyzed by SDS-PAGE and immunoblotted using the monoclonal ARF antibody 1D9. The results are given in Fig. 8. All fractions of the sucrose gradient contained membrane-bound ARF (Fig. 8 *A*, *upper panel*). When fractions 1–5 of the sucrose gradient were further separated on the Nycodenz gradient, ARF appeared mainly in fractions 1–3 (Fig. 8 *A*, *lower panel*). When the fractions of the Nycodenz gradient were analyzed additionally in a ligand-binding blot assay for the binding of GTP[γ^{35}S], a small GTP-binding protein of 20 kD was found to be enriched in fractions 1–3 (Fig. 8 *B*, *upper panel*). The corresponding Western blot (Fig. 8 *B*, *lower panel*) demonstrates that the small GTP-binding protein colocalizes with the signal obtained with the anti-ARF antibody 1D9. When GTP[α^{32}P] was used for detection of small GTP-binding proteins, the signal corresponding to the ARF protein was decreased, while that of other small GTP-binding proteins in fractions 5–7 (Fig. 8 *C*) was much more intense when compared to the GTP overlay using GTP[γ^{35}S]. Analysis of small GTP-binding proteins by 2-D gel electrophoresis and subsequent GTP[α^{32}P] ligand binding of the combined sedimented fractions 1–3 from the Nycodenz gradient showed that the small GTP-binding protein of 20 kD migrates as a single spot (Fig. 8 *D*). Comparison of a corresponding Western blot (using anti-ARF antibody 1D9) confirmed its identity as a member of the ARF family (data not shown). The additional small GTP-binding proteins of higher molecular weight found in the 2-D panel are caused by contaminations with SGBPs from the neighboring fractions (compare with Fig. 8 *C*).

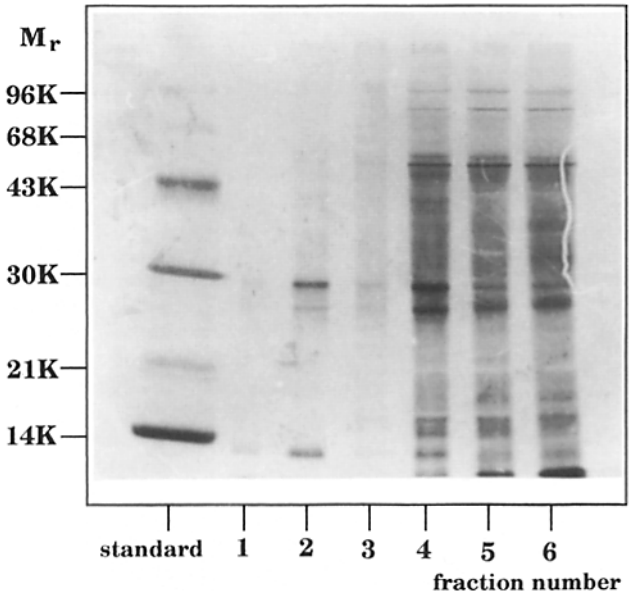

Figure 7. Proteins enriched in fractions containing purified post-TGN secretory vesicles (^{35}S-sulfated HSPG [4 min pulse, 8 min chase]). The amount of hepatocytes was as described in the legend to Fig. 1 *A*. Homogenization and subcellular fractionation by velocity-controlled sucrose centrifugation and Nycodenz equilibrium centrifugation were performed as described in the legends to Figs. 1 *A* and 4 *A*. Aliquots from fractions 1–6 of the final Nycodenz gradient were diluted 1:2 (vol/vol) with phosphate-buffered saline and particulate material sedimented by ultracentrifugation (100,000 *g*, 2 h). The sedimented material was processed by SDS-PAGE (13%) and subsequently silver-stained using standard procedures. A protein with an apparent molecular mass of ~14 kD was enriched in the first three fractions of the Nycodenz gradient (peak amount in fraction 2). The protein with an app. molecular mass of ~30 kD in fraction 2 was not always detected with a maximum in fractions 1–3. In fraction 4, proteins with similar electrophoretic mobility to VAPP14 and the 30-kD protein were detected. At the present time, it is not clear whether these proteins are identical to VAPP14 and the 30-kD protein, or whether they represent different proteins.

HSPG-carrying Secretory Vesicles do not Transport Albumin, Apolipoprotein E, and Fibrinogen

Since we had identified a post-TGN secretory vesicle carrying HSPGs, the question arose whether these vesicles contain also other proteins known to be constitutively secreted by hepatocytes. Analyzing the particulate material in the fractions of the Nycodenz gradient, RSA, apoE, and fibrinogen were detected in fractions 5–17 (Fig. 9 *A*), but not in fractions 1–3 containing the HSPG-carrying secretory vesicles.

This could mean that albumin, apoE, and fibrinogen become sorted in the TGN into different secretory vesicles than HSPGs. However, it could also mean that albumin is sorted into the same post-TGN vesicle as HSPG, but that this pool is very small and characterized by a very high turnover. Therefore, rat hepatocytes were pulse labeled with [^{35}S]-methionine. The experiments were performed at 32°C. Cells were analyzed after a pulse of 10 min and a subsequent chase for 0–60 min (Fig. 9 *B*). The cells were homogenized and further analyzed by sucrose velocity centrifugation followed by Nycodenz equilibrium density centrifugation as indicated in Materials and Methods. The vesicles of fractions 1–3 and of fractions 5–9 of the Nycodenz gradient were sedimented by ultracentrifugation, and the proteins were extracted and immunoprecipitated as indicated in Materials and Methods and in the legend to Fig. 9 *B*. Immunoprecipitates were separated by SDS-PAGE and analyzed by autoradiography (Fig. 9 *B*). At no time point ≤60 min chase time, radioactive albumin could be detected in fractions 1–3 of the Nycodenz gradient, which contained the HSPG-carrying post-TGN vesicles (Fig. 9 *B*, lane *1* in panels *a–f*). On the other hand, methionine became incorporated into albumin observed in fractions 5–9 of the Nycodenz gradient, which contained the maximum of the immunodetectable albumin (Fig. 9 *B*, lane *2* in panels *a–f*). The amount of radioactivity incorporated into albumin from fractions 5–9 increased up to a chase time of 15 min (pulse time plus chase time = 25 min) followed by a slow decrease. Under the conditions used (32°C incubation temperature), significant amounts of radioactive albumin did not appear in the medium after 20 min of chase (see legend to Fig. 9 *B*). After 30 and 60 min of chase time, increasing amounts of radioactive albumin could be detected in the medium (results not shown). These results can be explained best by assuming that HSPG on one hand, and albumin on the other hand, are sorted into different post-TGN secretory vesicles. These conclusions disagree with data earlier reported for rat liver post-TGN transport vesicles (Salamero et al., 1990).

Discussion

Characterization of the HSPG-carrying Post-TGN Vesicles

Here, we have identified and partially characterized a post-TGN vesicular fraction carrying HSPG in rat hepatocytes. As shown previously (Graham and Winterbourne, 1988), in rat hepatocytes, HSPG is transported exclusively to the plasma membrane and not to endosomal/lysosomal compartments. Therefore, the HSPG-transporting post-TGN vesicles described here are constitutive secretory vesicles. Post-TGN secretory vesicles have been first isolated and characterized in Madin-Darby canine kidney cells (Bennet et al., 1988; Wandinger-Ness et al., 1990). The density of these vesicles was found to be 1.099–1.113 g/ml, which is considerably higher than the density of the HSPG-carrying vesicles which was ~1.05–1.06 g/ml. On the other hand, the identification of HSPG-carrying secretory vesicles from rat hepatocytes as a low density compartment is in good agreement with the findings of Graham and Winterbourne (1988).

The most prominent protein associated with the HSPG-carrying secretory vesicles from rat liver during analysis by SDS-PAGE and silver staining was a small peripheral protein with an apparent molecular mass of 14 kD (VAPP14). We do not know yet whether this protein exchanges with free VAPP14 or with VAPP14 associated with other cellular compartments.

The only SGBP that was found to be associated with the HSPG-carrying secretory vesicles was a member of the ARF family. Since the monoclonal antibody 1D9 used in our studies reacts with multiple members of the ARF family, we do not know yet which specific member of the family of ARF proteins we are dealing with. A participation of ARF in the

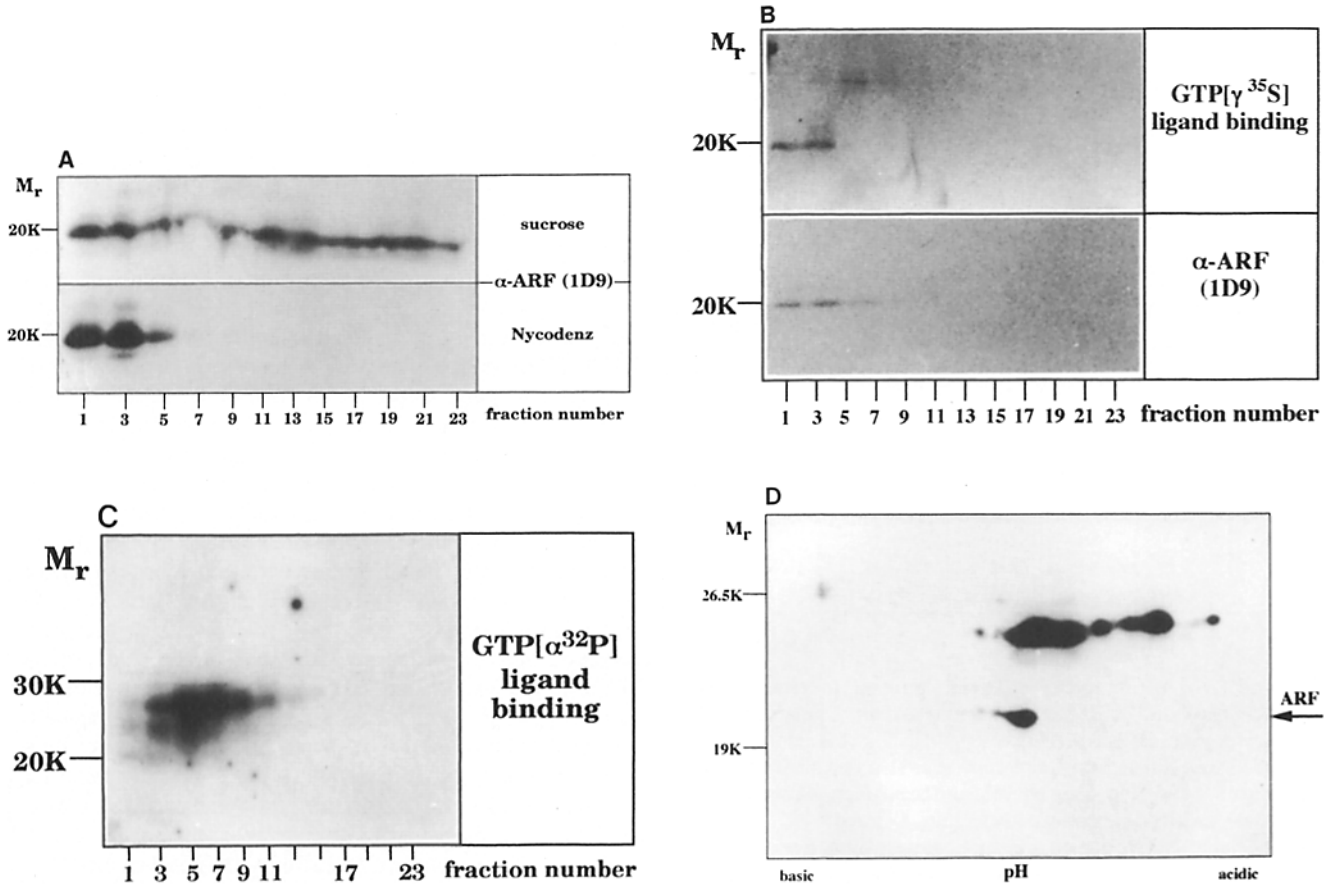

Figure 8. (*A*) Distribution of ARF in the velocity-controlled sucrose gradient and in the subsequent Nycodenz gradient as detected by the monoclonal antibody 1D9. The amount of hepatocytes was as described in the legend to Fig. 1 *A*. Homogenization and subcellular fractionation by velocity-controlled sucrose centrifugation and Nycodenz equilibrium centrifugation were performed as described in the legends to Figs. 1 *A* and 4 *A*. Aliquots from the indicated fractions of the gradients were diluted and particulate material sedimented by ultracentrifugation (100,000 *g*, 2 h) as given in Materials and Methods. The sedimented material was processed by SDS-PAGE (13%) and Western blotting. ARF was detected by the use of the monoclonal antibody 1D9. In the sucrose gradient (*upper panel*), ARF is distributed throughout the gradient. After Nycodenz gradient centrifugation (*lower panel*), ARF is only recovered in fractions 1–3, thus colocalizing with ^{35}S-labeled HSPG (4 min pulse, 8 min chase, compare with Fig. 4 *B*). (*B*) Identification of small GTP-binding proteins by GTP[γ^{35}S] ligand binding and immunodetection of ARF using the monoclonal antibody 1D9 in the Nycodenz gradient. The amount of hepatocytes was as described in the legend to Fig. 1 *A*. Homogenization and subcellular fractionation by velocity-controlled sucrose centrifugation and Nycodenz equilibrium centrifugation were performed as described in the legends to Figs. 1 *A* and 4 *A*. Aliquots from the indicated fractions of the gradient were diluted and particulate material sedimented by ultracentrifugation (100,000 *g*, 2 h). The sedimented material was processed by SDS-PAGE (13%) and Western blotting. *Upper panel*, GTP[γ^{35}S] ligand binding was performed; *lower panel*, the corresponding immune blot was used for the detection of ARF by the monoclonal anti-ARF antibody 1D9. The 20-kD signal obtained by GTP[γ^{35}S] ligand binding colocalizes with the signal generated with the anti-ARF antibody. (*C*) Detection of small GTP-binding proteins in the fractions of the Nycodenz gradient using GTP[α^{32}P] ligand binding. The amount of hepatocytes was as described in the legend to Fig. 1 *A*. Homogenization and subcellular fractionation by velocity-controlled sucrose centrifugation and Nycodenz equilibrium centrifugation were performed as described in the legends to Figs. 1 *A* and 4 *A*. Aliquots from the indicated fractions of the gradient were diluted and particulate material sedimented by ultracentrifugation (100,000 *g*, 2 h) as given in Materials and Methods. The sedimented material was processed by SDS-PAGE (13%) and Western blotting. GTP[α^{32}P] ligand binding was performed as described under Materials and Methods. The distribution of the 20-kD small GTP-binding protein (fractions 1–3) is identical to that seen after GTP[γ^{35}S] ligand binding. In contrast, the signal intensity is decreased. On the other hand, small GTP-binding proteins with molecular masses >20 kD show significantly stronger signals which extend also into fractions 1–3. (*D*) 2D-analysis of SGBPs in the pooled fractions 1–3 of the Nycodenz gradient. The amount of hepatocytes was as described in the legend to Fig. 1 *A*. Homogenization and subcellular fractionation by velocity-controlled sucrose centrifugation and Nycodenz equilibrium centrifugation were performed as described in the legends to Figs. 1 *A* and 4 *A*. The combined fractions 1–3 were diluted and particulate material sedimented by ultracentrifugation (100,000 *g*, 2 h) as given in the methods section. Sedimented material was processed by 2-D gel electrophoresis (Huber and Peter, 1993) and GTP[α^{32}P] ligand binding as described under Materials and Methods. After 2-D gel electrophoresis, the 20-kD small GTP binding protein detected after 1-D gel electrophoresis (see Fig. 8, *B* and *C*) migrated as a single spot. The position was the same as of ARF proteins detected with the monoclonal antibody 1D9 (data not shown). The additional small GTP-binding proteins of higher molecular mass are caused by contaminations from the neighboring fractions of higher density (compare with Fig. 8 *C*).

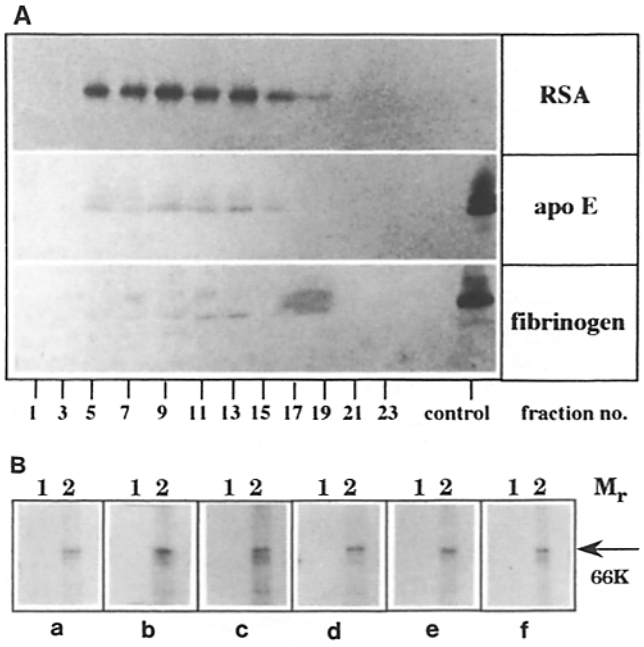

Figure 9. (*A*) Distribution of different secretory proteins under steady-state conditions in the Nycodenz gradient. The amount of hepatocytes was as described in the legend to Fig. 1 *A*. Homogenization and subcellular fractionation by velocity-controlled sucrose centrifugation and Nycodenz equilibrium centrifugation were performed as described in the legends to Figs. 1 *A* and 4 *A*. Aliquots from the indicated fractions of the gradient were diluted and particulate material sedimented by ultracentrifugation (100,000 *g*, 2 h) as given in Materials and Methods. The sedimented material was processed by SDS-PAGE (10%) and Western blotting. Polyclonal rabbit antibodies directed against RSA, apoE, and fibrinogen were used. These three proteins were distributed between fractions 5–17 and could not be detected in fractions containing HSPG-carrying secretory vesicles (fractions 1–3, see Fig. 4 *A*). (*B*) Pulse-chase labeling of hepatocytes using [^{35}S]methionine and subsequent immunoprecipitation of albumin from fractions of the Nycodenz gradient. Hepatocytes (150 mg/ml wet wt per experimental condition) were depleted of endogenous methionine by incubation for 60 min at 37°C in incubation medium supplemented with an amino acid-mixture lacking methionine (see Materials and Methods). The suspension was then transferred to 32°C and pulse labeled for 10 min with [^{35}S]methionine (100 μCi/ml). The chase period was started by addition of unlabeled methionine (2 mM final concentration) at 32°C for the times indicated below. Subsequently, cells were kept on ice to prevent any intracellular transport. Homogenization and subcellular fractionation by velocity-controlled sucrose centrifugation and Nycodenz equilibrium centrifugation was performed as given in the legends to Figs. 1 *A* and 4 *A*. Fractions 1–3 (lanes *1*) and fractions 5–9 (lanes *2*) of the Nycodenz gradient were pooled, diluted with PBS, and particulate material was sedimented by ultracentrifugation (100,000 *g*, 2 h) as described under Materials and Methods. Intravesicular material was extracted using PBS containing Triton X-100 (0.3%). After removal of insoluble material by ultracentrifugation, albumin was immunoprecipitated from the supernatant using a polyclonal antibody directed against rat serum albumin and Pansorbin®. The immunoprecipitates were processed by SDS-PAGE (10%) and the dried gels analyzed for [^{35}S]methionine incorporation by autoradiography. The chase times were as follows: *a*, 0 min; *b*, 5 min; *c*, 15 min; *d*, 25 min; *e*, 40 min; and *f*, 60 min. Under identical conditions, radiolabeled albumin did not appear in the medium ≤10 min of pulse plus 20 min of chase. After 30 min of chase, increasing amounts of radioactive albumin could be detected in the medium (data not shown).

vesicular transport from the ER to the Golgi (Balch et al., 1992) in intra-Golgi transport (Taylor et al., 1992), in endosome-endosome fusion (Lenhard et al., 1992), in TGN to late endosome transport (Stamnes and Rothman, 1993), as well as in the transport of nuclear membrane vesicles (Boman et al., 1992; Sullivan et al., 1993), has been shown. Here, it is demonstrated for the first time that a member of the family of ARF proteins is associated also with post-TGN secretory vesicles. This can explain previous observations, that Brefeldin A inhibits the formation of constitutive secretory vesicles from the TGN (Rosa et al., 1992; Miller et al., 1992). Brefeldin A was shown to inhibit the activity of a GDP/GTP exchange factor for ARF, which is necessary to allow ARF to bind to the donor membrane (Donaldson et al., 1992*b*; Helms and Rothman, 1992). Furthermore, ARF was shown to be involved in the binding of the coat protein β-COP to Golgi membranes (Donaldson et al., 1992*a*). Therefore, inhibition of the formation of constitutive secretory vesicles from the TGN by Brefeldin A implies the involvement of ARF. This is in line with the presence of ARF on this type of vesicles as presented in this study.

The HSPG-carrying post-TGN vesicles described here contained neither measurable amounts of the coat protein β-COP nor a visible coat structure, as assessed by electron microscopy. This by no means excludes that in the intact cells these vesicles possess a coat structure during and after budding from the TGN. In contrast to the conditions used for the isolation of intra-Golgi transport vesicles (Malhotra et al., 1989), we have isolated the vesicles in the absence of GTPγS. GTPγS is known to strongly inhibit the uncoating reaction. Therefore, the loss of a coat structure could be caused by the absence of GTPγS during the preparation of the vesicles.

Sorting of Secretory Proteins into Different Post-TGN Secretory Vesicles

In the Nycodenz gradient, vesicular structures containing the secretory proteins albumin, fibrinogen, or apolipoprotein E banded at higher densities than ^{35}S-sulfated HSPGs (4 min pulse, 8 min chase). The fractions containing these secretory proteins are most likely composed of a mixture of transport vesicles from different stages of the secretory pathway. In view of the almost undetectable traces of albumin associated with the HSPG-carrying vesicles, it seems unlikely that HSPG and albumin are sorted into the same post-TGN secretory vesicle.

Nevertheless, one cannot completely exclude the possibility that the post-TGN pool of secretory albumin is very small but has an extremely high turnover. However, when rat hepatocytes were pulse-labeled with [^{35}S]methionine (10 min) and chased for ≤60 min, labeled albumin could be detected in fractions 5–9 of the Nycodenz gradient, but at no time point in fractions 1–3, which contained the HSPG-carrying vesicles. The pulse-time of 10 min was adequately selected, especially considering the fact that the experiment was performed not at 37°C, but at 32°C. Since under these conditions, measurable amounts of radioactive albumin were not secreted earlier than 30 min after the chase, the lack of appearence of radiolabeled albumin in the HSPG-carrying vesicles cannot be explained by assuming that radiolabeled albumin had already left the pool of post-TGN secretory vesicles. Furthermore, radioactive albumin appeared in frac-

tions 5–9 already after a pulse of 10 min (Fig. 9 *B*). At this time point, labeled albumin could not be detected in the medium. Therefore, the labeled albumin observed in fraction 5–9 of the Nycodenz gradient can not represent secreted radioactive albumin that was subsequently endocytosed. At this point, the results are strongly indicative for a sorting of albumin and HSPG into different post-TGN secretory vesicles, although these data do not fit with those reported by others (Salamero et al., 1990). It is now necessary to also purify the albumin-containing constitutive secretory vesicles to characterize them with respect to cargo and vesicle associated proteins. This approach will also provide more information on the sorting mechanisms of constitutively secreted proteins in hepatocytes.

We are especially grateful to Sieglinde Zachmann and Heinz Hartmann (Zentrum Innere Medizin, Universität Göttingen, Germany) for help in preparing isolated rat hepatocytes. We thank Isabella Stefaner and Renate Fuchs (Institut für Allgemeine & Experimentelle Pathologie, Vienna, Austria) for help in identifying transcytotic vesicles, Klaus Oberbeck and David G. Robinson (Pflanzenphysiologisches Institut, Universität Göttingen, Germany) for the preparation of negative stained images of vesicular fractions, and Mrs. Dörler and Mrs. Neumann (Zentrum Innere Medizin, Universität Göttingen, Germany) for preparing electron micrographs of ultra-thin sections.

Received for publication 14 December 1993 and in revised form 4 February 1994.

References

Arouson, N. N., and O. Trouster. 1974. Isolation of rat liver plasma membrane fragments in isotonic sucrose. *Methods Enzymol.* 31:90–103.

Arvan, P., and J. D. Castle. 1982. Plasma membrane of the rat parotid gland: preparation and partial characterization of a fraction containing the secretory surface. *J. Cell Biol.* 95:8–19.

Baeuerle, P. A., and W. B. Huttner. 1987. Tyrosine sulfation is a *trans*-Golgi-specific protein modification. *J. Cell Biol.* 105:2655–2664.

Balch, W. E., R. A. Kahn, and R. Schwaninger. 1992. ADP-ribosylation factor is required for vesicular trafficking between the endoplasmic reticulum and the *cis*-Golgi compartment. *J. Biol. Chem.* 267:13053–13061.

Bennett, M. K., A. Wandinger-Ness, and K. Simons. 1988. Release of putative exocytic transport vesicles from perforated MDCK cells. *EMBO (Eur. Mol. Biol. Organ.) J.* 7:4075–4085.

Berry, M. N., and D. S. Friend. 1969. High yield preparation of isolated rat liver parenchymal cells. *J. Cell Biol.* 43:506–520.

Boman, A. L., T. C. Taylor, P. Melancon, and K. L. Wilson. 1992. A role for ADP-ribosylation factor in nuclear vesicle dynamics. *Nature (Lond.).* 358:512–514.

Brdiczka, D., D. Pette, G. Brunner, and F. Miller. 1968. Kompartimentierte Verteilung von Enzymen in Rattenlebermitochondrien. *Eur. J. Biochem.* 5:294–304.

Bucci, C., R. G. Parton, I. H. Mather, H. Stunnenberg, K. Simons, B. Hoflack, and M. Zerial. 1992. The small GTPase rab5 functions as a regulatory factor in the early endocytic pathway. *Cell.* 70:715–728.

Cameron, P. L., T. C. Südhof, R. Jahn, and P. De Camilli. 1991. Colocalization of synaptophysin with transferrin receptors: implications for synaptic vesicle biogenesis. *J. Cell Biol.* 115:151–164.

Carney, S. L., M. T. Bayliss, J. M. Collier, and H. Muir. 1986. Electrophoresis of ^{35}S-labeled proteoglycans on polyacrylamide-agarose composite gels and their visualization by fluorography. *Anal. Biochem.* 156:38–44.

Celis, J. E., B. Gesser, H. H. Rasmussen, P. Madsen, H. Leffers, K. Dejgaard, B. Honoré, E. Olsen, G. Ratz, J. B. Lauridsen, et al. 1990. Comprehensive 2D gel protein databases offer a global approach to the analysis of human cells: the transformed amnion cells (AMA) master database and its link to genome DNA sequence data. *Electrophoresis.* 11:989–1071.

Chavrier, P., R. G. Parton, H. P. Hauri, K. Simons, and M. Zerial. 1990. Localization of low molecular weight GTP binding proteins to exocytic and endocytic compartments. *Cell.* 62:317–329.

Donaldson, J. G., D. Cassel, R. A. Kahn, and R. D. Klausner. 1992*a*. ADP-ribosylation factor, a small GTP-binding protein, required for the binding of the coatomer protein β-COP to Golgi membranes. *Proc. Natl. Acad. Sci. USA.* 89:6408–6412.

Donaldson, J. G., D. Finazzi, and R. D. Klausner. 1992*b*. Brefeldin A inhibits Golgi membrane-catalysed exchange of guanine nucleotide onto ARF protein. *Nature (Lond.).* 360:350–352.

Fischer von Mollard, G., G. A. Mignery, M. Baumert, M. S. Perin, T. J. Hanson, P. M. Burger, R. Jahn, and T. C. Südhof. 1990. Rab3 is a small GTP binding protein exclusively localized to synaptic vesicles. *Proc. Natl. Acad. Sci. USA.* 87:1988–1992.

Fischer von Mollard, G., T. C. Südhof, and R. Jahn. 1991. A small GTP-binding protein dissocciates from synaptic vesicles during exocytosis. *Nature (Lond.).* 349:79–81.

Goud, B., A. Zahroui, A. Tavitian, and J. Saraste. 1990. Small GTP-binding protein associated with the Golgi cisternae. *Nature (Lond.).* 7:553–556.

Graham, J. M., and D. J. Winterbourne. 1988. Subcellular localization of the sulphation reaction of heparan sulphate synthesis and transport of the proteoglycan to the cell surface in rat liver. *Biochem. J.* 252:437–445.

Hall, C. W., I. Liebaers, P. Di Natale, and E. Neufeld. 1978. Enzymic diagnosis of the genetic mucopolysaccharide storage disorders. *Methods Enzymol.* 50:449–450.

Haubruck, H., R. Prange, C. Vorgias, and D. Gallwitz. 1989. The *ras*-related mouse YPT1 protein can functionally replace the YPT1 gene product in yeast. *EMBO (Eur. Mol. Biol. Organ.) J.* 8:1427–1432.

Helms, J. B., and J. E. Rothman. 1992. Inhibition by Brefeldin A of a Golgi membrane enzyme that catalyses exchange of guanine nucleotide bound to ARF. *Nature (Lond.).* 360:352–354.

Hoppe, C. A., T. P. Connoly, and A. L. Hubbard. 1985. Transcellular transport of polymeric IgA in the rat hepatocyte: biochemical and morphological characterization of the transport pathway. *J. Cell Biol.* 101:2113–2123.

Huber, L. A., S. Pimplikar, R. G. Parton, H. Virta, M. Zerial, and K. Simons. 1993. Rab 8, a small GTPase involved in vesicular traffic between the TGN and the basolateral plasma membrane. *J. Cell Biol.* 123:35–45.

Huber, L. A., and M. E. Peter. 1993. Mapping small GTP-binding proteins on high resolution two-dimensional gels by a combination of GTP-binding and labeling with *in situ* periodate-oxidized GTP. *Electrophoresis.* In press.

Kimura, J. H., L. S. Lohmander, and V. C. Hascall. 1984. Studies on the biosynthesis of cartilage proteoglycan in a model system of cultured chondrocytes from the swarm rat chondrosarcoma. *J. Cell. Biochem.* 26:261–278.

Kurzchalia, T. V., P. Dupree, R. G. Parton, R. Kellner, H. Virta, M. Lehnert, and K. Simons. 1992. VIP21, a 21-kD membrane protein is an integral component of *trans*-Golgi network-derived transport vesicles. *J. Cell Biol.* 118:1003–1014.

Laemmli, U. K. 1970. Cleavage of structural proteins during assembly of the head of bacteriophage T4. *Nature (Lond.).* 227:680–685.

Lenhard, J. M., R. A. Kahn, and P. D. Stahl. 1992. Evidence for ADP-ribosylation factor (ARF) as a regulator of in vitro endosome-endosome fusion. *J. Biol. Chem.* 267:13047–13052.

Luzio, J. P., B. Brake, G. Banting, K. E. Howell, P. Braghetta, and K. K. Stanley. 1990. Identification, sequencing and expression of an integral membrane protein of the *trans*-Golgi network (TGN38). *Biochem. J.* 270:97–102.

Malhotra, V., T. Serafini, L. Orci, J. C. Shepherd, and J. E. Rothman. 1989. Purification of a novel class of coated vesicles mediating biosynthetic transport through the Golgi stack. *Cell.* 58:329–336.

Maycox, P. R., E. Link, A. Reetz, S. A. Morris, and R. Jahn. 1992. Clathrin-coated vesicles in nervous tissue are involved primarily in synaptic vesicle recycling. *J. Cell Biol.* 118:1379–1388.

Miller, S. G., L. Carnell, and H. P. H. Moore. 1992. Post-Golgi membrane traffic: Brefeldin A inhibits export from distal Golgi compartment to the cell surface but not recycling. *J. Cell Biol.* 118:267–283.

Nakano, A., and M. Muramatsu. 1989. A novel GTP-binding protein, Sar1p, is involved in transport from the endoplasmic reticulum to the Golgi apparatus. *J. Cell Biol.* 109:2677–2691.

Peter, F., P. Nguyen Van, and H. D. Söling. 1992. Different sorting of Lys-Asp-Glu-Leu proteins in rat liver. *J. Biol. Chem.* 267:10631–10637.

Posner, B. I., M. N. Khan, and J. J. M. Bergeron. 1985. Peptide hormone receptors in intracellular structures from rat liver. *Methods Enzymol.* 109:223.

Reaves, B., M. Horn, and G. Banting. 1993. TGN38/41 recycles between the cell surface and the TGN: brefeldin A affects its rate of return to the TGN. *Mol. Biol. Cell.* 4:93–105.

Robinson, D. G., U. Ehlers, R. Herken, F. Mayer, and F. W. Schürmann. 1985. Präparationsmethodik in der Elektronenmikroskopie. Springer Verlag, Berlin.

Rosa, P., F. A. Barr, J. C. Stinchcombe, C. Binacchi, and W. B. Huttner. 1992. Brefeldin A inhibits the formation of constitutive secretory vesicles and immature secretory granules from the *trans*-Golgi network. *Eur. J. Cell Biol.* 59:265–274.

Salamero, J., E. S. Sztul, and K. E. Howell. 1990. Exocytic transport vesicles generated in vitro from the *trans*-Golgi network carry secretory and plasma membrane proteins. *Proc. Natl. Acad. Sci. USA.* 87:7717–7721.

Salminen, A., and P. J. Novick. 1987. A *ras*-like protein is required for a post-Golgi event in yeast secretion. *Cell.* 49:527–538.

Scheele, G., R. Jacoby, and T. Carne. 1980. Mechanism of compartmentation of secretory proteins: transport of exocrine pancreatic proteins across the microsomal membrane. *J. Cell Biol.* 87:611–628.

Schmitt, H. D., M. Puzicha, and D. Gallwitz. 1988. Study of a temperature-sensitive mutant of the *ras*-related YPT1-gene product in yeast suggests a role in regulation of intracellular calcium. *Cell.* 53:635–647.

Schweizer, A., J. A. M. Fransen, T. Bachi, L. Ginsel, and H. P. Hauri. 1988. Identification, by a monoclonal antibody, of a 53-kD protein associated with a tubulo-vesicular compartment at the *cis* side of the Golgi apparatus. *J. Cell*

Biol. 107:1643–1653.
Segev, N., J. Mulholland, and D. Botstein. 1988. The yeast GTP-binding YPT1 protein and a mammalian counterpart are associated with the secretion machinery. *Cell.* 52:915–925.
Seglen, P. O. 1974. Autoregulation of glycolysis respiration, gluconeogenesis and glycogen synthesis in isolated parenchymal rat liver cells under aerobic and anaerobic conditions. *Biochim. Biophys. Acta.* 388:317–336.
Stamnes, M. A., and J. E. Rothman. 1993. The binding of AP-1 clathrin adaptor particles to Golgi membranes requires ADP-ribosylation factor, a small GTP binding protein. *Cell.* 73:999–1005.
Stearns, T., M. C. Willingham, D. Botstein, and R. A. Kahn. 1990. ADP-ribosylation factor is functionally and physically associated with the Golgi complex. *Proc. Natl. Acad. Sci. USA.* 87:1238–1242.
Südhof, T. C., and R. Jahn. 1991. Proteins of synaptic vesicles involved in exocytosis and membrane recycling. *Neuron.* 6:665–677.
Sullivan, K. M. C., W. B. Busa, and K. L. Wilson. 1993. Calcium mobilization is required for nuclear vesicle fusion in vitro: implications for membrane traffic and IP3 receptor function. *Cell.* 73:1411–1422.
Taylor, T. C., R. A. Kahn, and P. Melancon. 1992. Two distinct members of the ADP-ribosylation factor family of GTP-binding proteins regulate cell-free intra-Golgi transport. *Cell.* 70:69–79.
Tooze, S. A., and W. B. Huttner. 1990. Cell-free protein sorting to the regulated and constitutive secretory pathways. *Cell.* 60:837–847.
Van der Sluijs, P., M. Hull, A. Zahraoui, A. Tavitian, B. Goud, and I. Mellman. 1991. The small GTP-binding protein rab4 is associated with early endosomes. *Proc. Natl. Acad. Sci. USA.* 88:6313–6317.
Verdon, B., and E. G. Berger. 1983. Galactosyl-transferase. *Methods Enzymol. Anal.* 3:374–381.
Wandinger-Ness, A., M. K. Bennett, C. Antony, and K. Simons. 1990. Distinct transport vesicles mediate the delivery of plasma membrane proteins to the apical and basolateral domains of MDCK cells. *J. Cell Biol.* 111:987–1000.
Zahraoui, A., N. Touchot, P. Chardin, and A. Tavitian. 1989. The human Rab genes encode a family of GTP-binding proteins related to the yeast YPT1 and SEC4 products involved in secretion. *J. Biol. Chem.* 264:12394–12401.